



UNIVERSITY OF LEEDS

This is a repository copy of *An investigation on process of seeded granulation in a continuous drum granulator using DEM*.

White Rose Research Online URL for this paper:
<http://eprints.whiterose.ac.uk/113300/>

Version: Accepted Version

Article:

Behjani, MA, Rahmanian, N, Ghani, NFBA et al. (1 more author) (2017) An investigation on process of seeded granulation in a continuous drum granulator using DEM. *Advanced Powder Technology*, 28 (10). pp. 2456-2464. ISSN 0921-8831

<https://doi.org/10.1016/j.appt.2017.02.011>

© 2017 The Society of Powder Technology Japan. Published by Elsevier B.V. and The Society of Powder Technology Japan. This manuscript version is made available under the CC-BY-NC-ND 4.0 license <http://creativecommons.org/licenses/by-nc-nd/4.0/>

Reuse

Unless indicated otherwise, fulltext items are protected by copyright with all rights reserved. The copyright exception in section 29 of the Copyright, Designs and Patents Act 1988 allows the making of a single copy solely for the purpose of non-commercial research or private study within the limits of fair dealing. The publisher or other rights-holder may allow further reproduction and re-use of this version - refer to the White Rose Research Online record for this item. Where records identify the publisher as the copyright holder, users can verify any specific terms of use on the publisher's website.

Takedown

If you consider content in White Rose Research Online to be in breach of UK law, please notify us by emailing eprints@whiterose.ac.uk including the URL of the record and the reason for the withdrawal request.



eprints@whiterose.ac.uk
<https://eprints.whiterose.ac.uk/>

An Investigation on Process of Seeded Granulation in a Continuous Drum Granulator Using DEM

Mohammadreza Alizadeh Behjani², Nejat Rahmanian^{1,*}, Nur Fardina bt Abdul Ghani³, Ali Hassanpour²

¹Chemical Engineering Programme, School of Engineering, Faculty of Engineering and informatics, University of Bradford, Bradford, BD7 1DP, UK.

²School of Chemical and Process Engineering, University of Leeds, Leeds, LS2 9JT, UK.

³Chemical Engineering Department, Universiti Teknologi PETRONAS, Tronoh 31750, Perak, Malaysia

^{1,*}Corresponding author email: n.rahmanian@bradford.ac.uk; +441274234552

ABSTRACT

Numerical simulation of wet granulation in a continuous granulator is carried out using Discrete Element Method (DEM) to discover the possibility of formation of seeded granules in a continuous process with the aim of reducing number of experimental trials and means of process control. Simple and scooped drum granulators are utilized to attain homogenous seeded granules in which the effects of drum rotational speed, particles surface energy, and particles size ratio are investigated. To reduce the simulation time a scale-up scheme is designed in which a dimensionless number (Cohesion number) is defined based on the work of cohesion and gravitational potential energy of the particles. Also a mathematical/numerical method along with a MATLAB code is developed by which the percentage of surface coverage of each granule is predicted precisely. The results show that use of continuous granulator is promising provided that a high level of shear is considered in the granulator design, i.e. using baffles inside drum granulators is essential for producing seeded granules. It is observed that the optimum surface energy for seeded granulation in scooped granulator (used in this study) with rotational speed of 50 rpm is 3 J/m^2 , which is close to the value predicted by the concept of Cohesion number. It is also shown that increasing the seed/fine size ratio enhances the seeded granulation both quantitatively (60% increase in seeds surface coverage) and qualitatively (more homogeneous granules).

Keywords: seeded granules, drum granulator, Discrete Element Method, surface energy, coordination number, cohesion number, scale up method

I. INTRODUCTION

Granulation process, simply defined as particle enlargement, is the process of collecting particles together by creating bonds between them in which the bonds can be formed by compression or using binding agent [1]. There are several obvious reasons indicating the significance of formation of these granules among which the improvement of materials properties and performance, e.g. increasing the flowability and reduction in dustiness, is of the highest importance. However, achieving a high degree of uniformity in product properties during granulation process is crucial and challenging. Extensive efforts have been made in the last decades to gain fundamental understanding of the wet granulation process in the batch granulators with focus on granule size distribution especially for pharmaceutical applications; yet, little attention

has been paid to the continuous process specially the internal structure of granules [2]. It is thus necessary to look more into continuous process simply because it has a significant potential to overcome the drawbacks associated with batch process and offers numerous advantages [3-5]. DEM modelling as a robust numerical method can help the manufacturers to have a better understanding of the mechanisms behind the continuous granulation.

A. Background

There are numbers of techniques available in granulation to combine the seeds and fine particles into required granulated form among which the most common methods are wet, dry, and melt granulation techniques [6] and these methods could be utilized in batch or continuous processes. Batch process in granules production industries undeniably offers many advantages with respect to quality assurance due to the fact that a batch is either accepted or rejected by quality inspections. However, there are some disadvantages combined with this method, e.g. the challenge of process scale-up and high operation costs. Considerable efforts have been made in the past years to gain fundamental understanding of scale-up characteristics in batch granulators and the impacts on granules [7, 8]; however, many researchers have preferred to overcome the scale up issue by employing other alternatives of the batch production such as continuous and semi-continuous processes. As a result, number of studies regarding the replacement of batch with the continuous method is increasing day by day [9, 10].

B. Seeded Granulation

The term of “seeded granulation”, for the first time, was used by Rahmanian et al. [11, 12] through which they described a new method of granulation confirmed to assure producing consistent granule structure and properties. This seeding mechanism occurs when larger particles, usually known as seeds, become partially wetted, act as a nucleus at the granules core, and finally get covered by finer particles. As a result, particles accumulate around the seed, adhere to each other, and form the seeded granules (Figure 1). It is also observed by Rahmanian et al. [12] that two factors strongly affecting and contributing to the formation of seeded granules in high shear mixer are the optimum impeller tip speed and the primary size distribution of the feed particles. Based on these parameters, a regime map, displaying the preferable conditions for seeded granules formation, is established for the Cyclomix batch granulator (Figure 2.). Since the aforementioned investigations are related to batch processes, it is thus highly desirable to further analyse the mechanisms of formation of seeded granules within the continuous granulators to discover product-process relationship. This work in essence is in line with the previous work by Rahmanian and Ghadiri [13] for taking the advantage of DEM to optimise the formation of seeded granules in continuous granulators. A numerical investigation over the seeded granulation in batch granulators has already been accomplished by Hassanpour et al. [14], therefore the main focus of this study is on DEM

simulation of granulation of Calcium Carbonate powder in continuous granulators to analyse the flow and mixing behaviour of particles due to different operating parameters.

II. METHODOLOGY

A. Discrete Element Method (DEM)

In recent years numerical techniques based on discrete approaches, aimed to simulate the behaviour of particulate materials, have been rapidly developed worldwide mainly as the result of significant enhancement in computers' processing capabilities. DEM is probably the most fast developing mathematical model in recent decades to model the granular materials and processes [15]. The superiority of DEM over other numerical methods in this study lies on its capability of applying precise contact models for modelling particles collisions and cohesivity in addition to the fact that individual particles are trackable. With the aid of DEM, the formation and depletion of granules are easily observed and the quality and durability of the seeded granules can be assessed [2, 16-19].

B. Contact Model

DEM simulations of the continuous granulation process are conducted utilizing EDEM 2.7.0 software provided by DEM Solutions, Edinburgh, UK. The models used for particles contacts are Hertz-Mindlin [20-22] and JKR [20] by which both the effects of collisions and cohesion are taken into consideration. Hertz-Mindlin theory is basically used in case of collision between two particles; where the Hertz theory [21] calculates the normal component of the contact force and the Mindlin theory [22] determines the tangential component. The details of these models are available in other articles [23, 24]. Any surface interactions such as van der Waals or contact adhesive interactions are neglected in this theory; therefore to simulate the cohesion force between particles, Hertz-Mindlin with the JKR model is employed. To justify the applicability of the JKR model in this study, Tabor's coefficient [25] is determined for the experimental case published by Rahmanian et al. [12]. This coefficient varies roughly between 1.0 and 3.0, and based on what Tabor addresses, the JKR model is applicable for this study. Bonding forces in wet granulation are due to the both surface tension and viscous forces. The surface tension forces are considered by implementing the particles surface energy in the JKR model and to account for viscous dissipation, a low restitution coefficient is selected [14].

Cohesion number

JKR model is basically an extent for the Hertz model in which adhesive force between the particles is also taken into account; however, the contact area in JKR is bigger than that of the Hertz so there is a circular compressive zone inside a bigger circle which tolerates tensile force after the particles are released from compression. In JKR model, the attractive

forces between particles are limited just to the contact zone and are basically assumed to be short range. Figure 3 shows how the JKR model predicts the force-overlap response during an elastic-adhesive contact. Considering two spheres approaching each other, when they come close enough, their normal force drops to $\frac{8}{9}F_C$ due to van der Waals force, where F_C is the pull-off force [26]. Then because of the initial velocities of the two spheres towards each other a positive overlap happens and particles kinetic energies gradually convert to elastic potential energy until their velocities become zero. At the loading stage, spheres experience maximum compression at zero velocity after which the kinetic energy is fully recovered by conversion of the elastic potential energy into kinetic energy. Therefore, the spheres velocities increase until their overlap becomes zero; however at this stage, the particles do not detach owing to the adhesive force. The adhered particles then experience a tensile force and lose kinetic energy until fully depart with a negative overlap of α_F at $F = \frac{5}{9}F_C$. The work needed to break the contact and detach the spheres is known as the work of cohesion and is shown by the shaded area in Figure 3.

The pull-off force is the maximum tensile force that the spheres experience and is given by the following equations,

$$F_C = \frac{3}{2}\pi R^* \Gamma \quad (1)$$

$$R^* = \left(\frac{1}{R_1} + \frac{1}{R_2}\right)^{-1} \quad (2)$$

where R_1 and R_2 are particles radii, R^* is the equivalent radius, and Γ is the surface energy of the particles. Also work of cohesion needed to detach the spheres is given by the equation (3).

$$W_C = 7.09 \left(\frac{\Gamma^5 R^{*4}}{E^{*2}}\right)^{1/3} \quad (3)$$

$$E^* = \left(\frac{1-\nu_1^2}{E_1} + \frac{1-\nu_2^2}{E_2}\right)^{-1} \quad (4)$$

where E^* is the equivalent Young's modulus of elasticity of the spheres, E_1 and E_2 are Young's moduli of the spheres and ν_1 and ν_2 are Poisson's ratios of their materials, respectively [26].

In DEM modelling due to high computation time, it is common to utilize larger particles with lower value of Young's modulus; however, there should be a basis for this scale up so that the right value of surface energy is coordinated with the particles size and mechanical properties. To fulfil this, a dimensionless number is suggested which is based on the ratio of work of cohesion over the particles gravitational potential energy with regards to a characteristic height equal to the equivalent radius defined previously.

The free body diagram of the particles and the normal forces existing on each one are depicted in Figure 4.

Based on this, the dimensionless number is derived as follows:

$$\text{Cohesion number} = \frac{\text{Work of cohesion}}{\text{Gravitational potential energy}}$$

$$\text{Coh} = \frac{7.09 \left(\frac{\Gamma^5 R^{*4}}{E^{*2}} \right)^{1/3}}{mgR^*} \quad (5)$$

By substituting the mass by density times the volume and eliminating the constant coefficients, the equation (5) will be:

$$\text{Coh} = \frac{\left(\frac{\Gamma^5 R^{*4}}{E^{*2}} \right)^{1/3}}{\rho R^{*3} g R^*} \quad (6)$$

Simplifying the equation (6), we will have the cohesion number as following:

$$\text{Coh} = \frac{1}{\rho g} \left(\frac{\Gamma^5}{E^{*2} R^{*8}} \right)^{1/3} \quad (7)$$

This number is then utilized to select the appropriate values of the surface energy and the shear modulus in DEM analysis with respect to the level of scale up selected.

C. Geometry and material properties of the particles

Material properties of seeds and fines used in the simulation are set in such a way that the cohesion numbers of both experimental case run by Rahmanian et al. [12] and the DEM simulation are in the same order. To do so, the particles size and shear modulus are selected with the aim of having less computation and avoiding large overlaps during the contacts and then the value of the surface energy is determined on this basis. Calcium Carbonate powder is utilized as the material to be granulated and aqueous Polyethylene Glycol (PEG) 4000 acts as the binder. The aforementioned particles properties are provided in Table 1. As an example the average surface energy of the PEG is 0.043 J/m² [27-29] mostly measured by the contact angle method. Using this value, the Cohesion number, shown in equation (7), is then calculated to be 0.316 and keeping this value constant, the equivalent surface energy to be used in DEM with larger particles and softer material is 2.1 J/m². On this basis a range of differing values of surface energy is defined in the simulations which is between 0.5 and 5 J/m².

The particles interactional properties are provided in Table 2. In this study, it is assumed that the binder has uniformly covered the particles, thus the model is applied for all the particles equally.

D. Drum Granulator Model

Geometry of the drum granulator is designed using AutoCAD 2007 software and exported to the EDEM 2.7.0. The geometrical parameters and dimensions of the granulator are listed in Table 3 and the granulator geometry is shown in Figure 5. As presented, there are two types of geometries utilized, one with baffles and the other without baffles, however, both are equal in dimensions. The idea of adding baffles to the simple drum comes from the fact that granules need to experience a high level of shear inside the drum which would be achieved by using baffles. In the first stage, simulations are executed using the simple drum and later, the scooped drum is also utilized to assess the effect of granulator design.

III. RESULTS AND DISCUSSION

This simulation is carried out by introducing mono-sized large and fine particles into the left end of the drum granulator with the aim of producing seeded granules. Particles are let to settle under the natural gravity force and this filling process happens simultaneously with rotation of the tilted drum. This process represents a continuous process through which the seeds and the fines are fed from the left inlet and led to the right by the driving force of gravity and tumblers rotation since the drum is tilted to the right. Particles are introduced into the system during the first 8 seconds and their number remains constant through the rest of the simulation to observe the effect of using a continuous granulation process as well as to see the effect of residence time on granulation quality. This simulation is carried out for three different drum rotational speeds (10, 50, and 100 rpm) each lasts for 20 seconds.

A. Effect of geometry design

In all types of the granulation and mixing, geometry and the shape of mixers have key role, hence it is of worth to do a study on the geometry of the granulator prior to further modelling. It is noteworthy that the granulator in this study was originally a simple drum in which seeds and fines were being introduced and meant to be mixed homogeneously. However, in order to investigate the effect of shear inside the granulator as well as particles residence time on the quality of granulation, adding baffles to the drum was suggested.

Figure 6 shows the snapshots of simulation progress at two different times, with drum rotational speed at 50 rpm and particle surface energy of 1.5 J/m^2 . The figures clearly show that most of the fines settle down at the bottom of the drum, whilst seed particles in red colour are on top of small particles. This segregation which is known as Brazil nut effect occurs due to the considerable difference in size of the particles and low quality of mixing [30, 31]. It is perceived from the snapshots that the particles relative positions stay unchanged during the 20 seconds of simulations.

The total number of immediate contacts between seeds and fine particles through the simulation time is demonstrated in Figure 7. This value can be used as a suitable indicator of the granulation and formation of seeded granules. It is observed that the number of contacts increases for all the cases between time 0 and 8 seconds which is expected on account of the increase in number of both fines and seeds during the introducing of the particles into the system; however after this period, the graphs show much less change and meet plateaus. One of the clear facts in the graphs is their smoothness before and after the 8th second implying that the number of contacts does not have fluctuations and variations during the process. It shows that apart from some minor movements in the particles mixture, the relative position of the seeds and fines does not differ through the process due to their stickiness. It is also observed that the number of contacts for different rotational speeds is not in order. The highest contact number is obtained at 10 rpm and the lowest number at 50 rpm.

The mixing patterns of particles at various feeding stages for differing rotational speeds of the drum is depicted in Figure 8. It is demonstrated that for the whole range of the granulator speed, there is an extent of segregation within the mixture as well as lack of enough relative movement and rolling of particles due to the granulator shape. For 10 rpm, all the seeds and fines introduced into the drum are piled near the entrance zone and hardly change position, thus the highest contact number is observed at this speed. However, this case cannot be considered as granulation and does not show enough evidence of seeded granules. For 50 rpm, on the other hand, the particles have small slips on the granulator wall helping them in moving forward and preventing them from being accumulated in one place. Clearly in this case the number of contacts is lower than that of the 10 rpm because the particles are spread through the granulator and seeds are not confined by the fines. If the speed is increased to 100 rpm, the particles rolling and relative movement increase, contributing in higher number of contacts.

To find out the effect of granulator geometry on granulation, the simulation work was then extended using a different design of granulator in which some scoops are attached to the inner side of the drum to enhance the efficiency of the granulator. As shown in Figure 9, the drum with scoops increases the kinetic energy of the particles immensely causing more contacts and rapid collisions between seeds and fines which can also be observed from Figure 10. This type of motion leads to rapid growth and breakage of the agglomerates which can be deduced from the fluctuations in number of contacts of the particles. At the end of the simulation, scooped granulator does not present a quantitative superiority over the simple granulator in terms of total seed-fine contact numbers; nevertheless, the seeded granules can be observed only in scooped granulators. As depicted in Figure 10, in scooped granulator, some of the seeds are nicely surrounded by the fines forming the first and second layers of the contacts; whereas in simple granulator, the particles are just piled over each other. It is concluded so far that using the baffles in the drum does not increase the total number of the seed-fine contacts; however,

it is necessary for delivering seeded granules throughout the process of granulation. On the other hand, in the simple drum the fines and seeds have merely simple contacts due to piling of the particles over each other which is not a firm proof of granules formation.

Percentage of seed coverage by the fines is a suitable criterion which can be utilized to compare the efficacy of the seeded granulations in continuous granulators in general and each case in specific. To find the coverage percentage, it is needed to find the number of fines attached to each seed as well as the coordination number of seeds with respect to the fine/seed size ratio. A MATLAB (R2014a) code is made by which the number of fines having immediate contact with each seed can be obtained. Coordination number is the maximum number of fines can be accommodated around a single seed. This value is determined using Euclidean geometry and mathematical methods in addition to taking the advantage of DEM modelling.

In theory, a properly seeded granule should have the seed fully covered with at least one layer of fine particles. Finding out the exact number of fine particles for full coverage of the seed is not easy as it has been one of the famous mathematical problems called the kissing number problem (coverage number) [32-35]; nevertheless, it is possible to estimate the number of covering particles by doing mathematical calculations. Based on our own mathematical and geometrical analysis, the maximum number of covering particles for this case is 88 ± 2 which is quite close to the prediction of Deiters [34] equal to 92. In our method, number of the particles (fines) covering the central particle (seed) is estimated based on the total surface area of a virtual sphere with a radius equal to the summation of the radii of central and covering particles over the area that a single particle occupies in a monolayer of packed covering particles. Having said that, this prediction is a theoretical one which hardly happens in reality, therefore to find the maximum number of particles for covering the seeds, a separate simulation is designed in which a single seed is placed and tumbled among the fines with high cohesivity between the seed and the fine particles. Figure 11 shows the image of one seed covered by fine particles in different percentages of coverage. It demonstrates how the number of contacts between the seed and fines is increased through the simulation time until the seed is fully covered and hence hidden within the fines. It is observed that for this particles size ratio, $d_{seed}/d_{fine}=4$, a seed can be considered as a fully covered particle when having 65 fines in contact. Since the simulation shows that full coverage for the seed is fulfilled by 65 fine particles and it is more realistic data compared to the mathematical one, the percentage of seed coverage will be calculated based on this number. In the next sub-section, further analysis of the simulation works is done accordingly by manipulating several variables such as granulator design, drum rotational speed, size ratio of the particles, and their surface energy.

B. Effect of Drum Rotational Speed

The total number of seed-fine contacts for both scooped and simple drums is shown in Figure 12. For the simple granulator, the highest number of contacts by far is achieved in 10 rpm reaching 750 contact numbers, while the lowest number is attained for the 50 rpm with 500 contacts and the results for 100 rpm lies between them equal to 600 contacts for 40 seeds. On the other hand, scooped granulator gives rather the same number of contacts for all the rotational speeds, especially after the 14th second of granulation process. It seems that for the simple granulators low rotational speeds lead to high number of contacts due to accumulation of the particles in one place while higher speeds contribute to spreading of particles and hence less number of contacts is achieved. As mentioned previously, although the total contact numbers for scooped granulator is less than that of the simple one, the scooped granulator shows better results in terms of formation of seeded granules and qualitative visualization of the granules.

Rahmanian et al. [12] showed that in batch granulator, the number of seeded granules depends on the impeller tip speed as well as the seed-fine size ratio. Based on their results, higher impeller speeds deliver better seeded granules; whereas for the continuous scooped granulator, it seems that the contact number does not noticeably depend on the rotational speed of the drum. The continuous process seems to have different behaviour from the batch operation since the geometry and speed range differs from those of the batch granulator. Being able to calculate the surface coverage for each seed, the percentage of seed coverage by fines is calculated and its distribution at $t=10s$ is depicted in Figure 13. Horizontal axis shows the level of surface coverage and the vertical axis displays the per cent of covered seeds in each coverage level (uniformity in granulation based on number of contacts). The highest level of uniformity in granulation is achieved in simple granulator at 100 rpm where 56% of the seeds are covered between 20-30%. The lowest coverage happens at scooped granulator with 50 rpm where most of the seeds have less than 20% coverage. However, scooped drum having 100 rpm has by far the highest number of seeds covered more than 30%. Also the only case in which more than 40% coverage is observed is in the scooped drum with 50 rpm. The uniformity achieved in simple drums is because of non-chaotic nature of mixing in simple drums as described in the previous section; nevertheless, adding baffles leads to rise in number of highly-covered seeds and higher possibility of seeded granulation.

C. Effect of Particle's Surface Energy

Based on JKR Theory, particles lose their kinetic energy after collision which appears in the form of speed reduction and is basically due to implementation of the surface energy. If this surface energy is high enough then the colliding particles lose their energy, achieve a zero relative velocity after collision and stick together to form the granules. The durability of this stickiness however depends on the size ratio of the particles, particles shape, and the shear stresses

imposed on the particles. It is believed that a greater value of particle's surface energy gives higher number of potential seeded granules owing to higher cohesion effect between particles; yet to be proved quantitatively.

Granulation of seeds and fines is simulated in the scooped granulator with the rotational speed of 50 rpm for four different cases having differing surface energies. Figure 14 shows the contact number of these four cases with surface energies equal to 0.5, 1.5, 3.0, and 5.0 J/m². For the 0.5 J/m², the contacts number increases gradually from zero in the beginning to 300 at the 20th second with the average of 200. This average number is nearly two times higher when surface energy is 1.5 J/m² and 3.5 times higher for the 3.0 and 5.0 J/m² surface energies. As expected, increasing the surface energy raises the number of contacts in granulator; however, augmenting the surface energy has a limited effect on the granulation since for the two last cases of 3.0 and 5.0 J/m² the results are pretty much the same apart from some minor fluctuations. The snapshots of the seeded granules inside the drum are also displayed in Figure 15. It is evident that seeded granules do not form in the first case (0.5 J/m²); instead, the finer particles are segregated in the outer layer of the mixture while the seeds are closer to the centre of the drum. However, the second and third cases (1.5 and 3.0 J/m²) display some well-covered seeds which is a promising outcome. Having said that, increasing the surface energy from 3 to 5 J/m², not only has insignificant effect on the number of contacts but also leads to coagulation of the particles and deteriorates the granulation.

D. Effect of Seed/ Fine Size Ratio

Size ratio of the seeds and fines is an important parameter that should be taken into consideration. If the size difference increases, naturally, the seeds can accommodate more fines on their surfaces; however for a better comparison, it is needed to know the coordination number of the new seed-fine arrangement and then divide the total contact numbers by the coordination number to have a dimensionless number which gives a suitable comparison for the coverage area of the seeds. For this purpose, the size ratio of seeds and fines is increased from 4 to 8 by reducing the fines diameter to 1 mm and keeping the seeds diameter unchanged. To maintain the conditions of the simulation similar to the previous ones, the same volume of the fine particles is introduced into the granulator which means that the number of fines is increased 8 times equals to 32000.

The theoretical coordination number of the new size ratio (8:1) is approximately 291 ± 2 which is 3.3 times greater than that of 4:1 size ratio. Hence, the total contact numbers are divided by the coordination numbers and are presented in the Figure 16 as the term contact ratio. It is observed that for the 4:1 size ratio, contact ratio increases through the time until all the particles are introduced into the granulator and from $t=8$ s until the end of simulation the contact ratio fluctuates between 5 and 6. On the other hand, contact ratio for the 8:1 size ratio case increases even after the 8th second and rises up to 8.5 with a decelerating rate till the $t=16$ s which then meets a plateau. This graph proves that the probability of formation

of seeded granules is higher when finer particles are used with the same seeds size; in other words, the higher the size ratio is, the better granules form. This statement is also evident in Figure 17 where utilizing the particles with size ratio of 8:1, has increased the number of granules categorized in 10-40 percent coverage zone at $t=10$ s indicating well-covered and homogenous granules. To add to the benefit of using higher size ratios, continuing the granulation for more 10 seconds has led to achieving a state in which 50% of the seeds have the 30-40 percent coverage. As a result, there is a significant promise in increasing the quality of the seeded granules by employing higher seed-fine size ratios.

IV. CONCLUSION

Process of seeded granulation in a continuous drum granulator is simulated using DEM. The effects of granulator geometry, particles size ratio, granulator rotational speed, and particles surface energy on granules quality are investigated. A dimensionless number termed as Cohesion number is suggested by which the simulated process can be scaled up. Also the total number of contacts and the surface coverage of individual seeds are calculated by mathematical and numerical methods. It is observed that continuous granulators with the baffles have reasonable potential of being used in seeded granulation process. It is also demonstrated that particles tend to segregate inside the simple drum and stick to each other after segregation, whereas the scooped granulator uniforms the granulation effectively.

Using Cohesion number, it is possible to determine the value of surface energy to be utilized in DEM modelling with respect to the material properties in the experiment. For example, the optimum value of surface energy in the modelling is observed to be 3 J/m^2 which is close to the estimation of the Cohesion number. It is also observed that the seed-fine size ratio plays a key role in formation of seeded granules, i.e. increasing the size ratio promotes the seeded granulation. Using the coordination number of the seed, the surface coverage of the seeds by fines is calculated indicating that between 10 to 50 percent of the seeds surfaces are covered by fines with direct contacts and the rest of the fines have indirect contact with the seeds. In scooped granulator, particles surface energy and size ratio have high impact on contact number; however, granulator speed is not as influential.

On the basis of doing this research, more research in this area is highly recommended. The effects of new types of continuous granulators, seed to fine size ratio and feeding ratio, shape of the particles, residence time, particles size distribution, binder properties, and binder concentration are all important.

ACKNOWLEDGEMENT

The work presented here was firstly initiated at the Universiti Teknologi PETRONAS where the corresponding author did the research and also presented the work in 5th Asian Particle Technology Forum [36]. The work was later on extended, adapted and modified in the current form in collaboration with the University of Leeds.

REFERENCES

- [1] S.M. Iveson, J.D. Litster, K. Hapgood, B.J. Ennis, Nucleation, growth and breakage phenomena in agitated wet granulation processes: a review, *Powder Technology*, 117 (2001) 3-39.
- [2] A. Kumar, K.V. Gernaey, T. De Beer, I. Nopens, Model-based analysis of high shear wet granulation from batch to continuous processes in pharmaceutical production - A critical review, *Eur J Pharm Biopharm*, 85 (2013) 814-832.
- [3] J. Vercruyse, E. Peeters, M. Fonteyne, P. Cappuyns, U. Delaet, I. Van Assche, T. De Beer, J.P. Remon, C. Vervaet, Use of a continuous twin screw granulation and drying system during formulation development and process optimization, *Eur J Pharm Biopharm*, 89 (2015) 239-247.
- [4] M.A. Jarvinen, M. Paavola, S. Poutiainen, P. Itkonen, V. Pasanen, K. Uljas, K. Leiviska, M. Juuti, J. Ketolainen, K. Jarvinen, Comparison of a continuous ring layer wet granulation process with batch high shear and fluidized bed granulation processes, *Powder Technology*, 275 (2015) 113-120.
- [5] P. Beer, D. Wilson, Z.Y. Huang, M. De Matas, Transfer from High-Shear Batch to Continuous Twin Screw Wet Granulation: A Case Study in Understanding the Relationship Between Process Parameters and Product Quality Attributes, *J Pharm Sci-U.S.*, 103 (2014) 3075-3082.
- [6] H.G. Kristensen, T. Schaefer, Granulation: A Review on Pharmaceutical Wet-Granulation, *Drug Development and Industrial Pharmacy*, 13 (1987) 803-872.
- [7] A. Hassanpour, C.C. Kwan, B.H. Ng, N. Rahmanian, Y.L. Ding, S.J. Antony, X.D. Jia, M. Ghadiri, Effect of granulation scale-up on the strength of granules, *Powder Technology*, 189 (2009) 304-312.
- [8] N. Rahmanian, B.H. Ng, A. Hassanpour, Y.L. Ding, S.J. Antony, X.D. Jia, M. Ghadiri, P.G.J. van der Wel, A. Krug-Polman, D. York, A. Bayly, H.S. Tan, Scale-up of High-Shear Mixer Granulators, *Kona Powder Part J*, 26 (2008) 190-204.
- [9] G. Betz, P. Junker-Burgin, H. Leuenberger, Batch and continuous processing in the production of pharmaceutical granules, *Pharm Dev Technol*, 8 (2003) 289-297.
- [10] C. Vervaet, J.P. Remon, Continuous granulation in the pharmaceutical industry, *Chem Eng Sci*, 60 (2005) 3949-3957.
- [11] N. Rahmanian, M. Ghadiri, Comment of the Cover Photograph Seeded Granulation, *Kona Powder Part J*, (2011) 3-3.
- [12] N. Rahmanian, M. Ghadiri, X. Jia, Seeded granulation, *Powder Technol*, 206 (2011) 53-62.
- [13] N. Rahmanian, M. Ghadiri, Strength and structure of granules produced in continuous granulators, *Powder Technology*, 233 (2013) 227-233.
- [14] A. Hassanpour, M. Pasha, L. Susana, N. Rahmanian, A.C. Santomaso, M. Ghadiri, Analysis of seeded granulation in high shear granulators by discrete element method, *Powder Technology*, 238 (2013) 50-55.
- [15] A.-N. Huang, H.-P. Kuo, Developments in the tools for the investigation of mixing in particulate systems – A review, *Adv Powder Technol*, 25 (2014) 163-173.
- [16] N. Deen, M.V.S. Annaland, M. Van der Hoef, J. Kuipers, Review of discrete particle modeling of fluidized beds, *Chem Eng Sci*, 62 (2007) 28-44.
- [17] C. Wassgren, J.S. Curtis, The application of computational modeling to pharmaceutical materials science, *Mrs Bull*, 31 (2006) 900-904.
- [18] H.P. Zhu, Z.Y. Zhou, R.Y. Yang, A.B. Yu, Discrete particle simulation of particulate systems: Theoretical developments, *Chem Eng Sci*, 62 (2007) 3378-3396.
- [19] H.P. Zhu, Z.Y. Zhou, R.Y. Yang, A.B. Yu, Discrete particle simulation of particulate systems: A review of major applications and findings, *Chem Eng Sci*, 63 (2008) 5728-5770.
- [20] K.L. Johnson, K. Kendall, A.D. Roberts, Surface Energy and the Contact of Elastic Solids, *Proceedings of the Royal Society of London A: Mathematical, Physical and Engineering Sciences*, 324 (1971) 301-313.

- [21] H. Hertz, Ueber die Berührung fester elastischer Körper (on the contact of elastic solids), in: *Journal für die reine und angewandte Mathematik (Crelle's Journal)*, 1882, pp. 156–171.
- [22] H. Deresiewicz, R.D. Mindlin, U. Columbia, E. Department of Civil, Elastic spheres in contact under varying oblique forces, 1952.
- [23] A. Di Renzo, F.P. Di Maio, Comparison of contact-force models for the simulation of collisions in DEM-based granular flow codes, *Chemical Engineering Science*, 59 (2004) 525-541.
- [24] M.M. Martín, *Introduction to software for chemical engineers*, CRC Press, 2014.
- [25] D. Tabor, Surface forces and surface interactions, *J Colloid Interf Sci*, 58 (1977) 2-13.
- [26] C. Thornton, Z. Ning, A theoretical model for the stick/bounce behaviour of adhesive, elastic-plastic spheres, *Powder Technol*, 99 (1998) 154-162.
- [27] A. Agrawal, *Surface Tension of Polymers (lecture notes)*, in, Department of Mechanical Engineering, Massachusetts Institute of Technology, MIT, 2005, pp. 1-29.
- [28] K. Van Ness, Surface tension and surface entropy for polymer liquids, *Polymer Engineering & Science*, 32 (1992) 122-129.
- [29] C.J. van Oss, M.K. Chaudhury, R.J. Good, Monopolar surfaces, *Adv Colloid Interfac*, 28 (1987) 35-64.
- [30] Y.Z. Zhao, M.Q. Jiang, J.Y. Zheng, Discrete element simulation of the segregation in Brazil nut problem, *Acta Phys Sin-Ch Ed*, 58 (2009) 1812-1818.
- [31] A. Rosato, K.J. Strandburg, F. Prinz, R.H. Swendsen, Why the Brazil nuts are on top: Size segregation of particulate matter by shaking, *Phys Rev Lett*, 58 (1987) 1038-1040.
- [32] S. Kucherenko, P. Belotti, L. Liberti, N. Maculan, New formulations for the Kissing Number Problem, *Discrete Applied Mathematics*, 155 (2007) 1837-1841.
- [33] G.H. Eduljee, C. McDermott, Estimating the maximum coordination number for spheres of different sizes, *Fluid Phase Equilibria*, 18 (1984) 103-108.
- [34] U.K. Deiters, "Coordination numbers for rigid spheres of different sizes—estimating the number of next-neighbour interactions in a mixture" by G.H. Eduljee, *Fluid Phase Equilibria*, 12 (1983) 193-197.
- [35] U.K. Deiters, Coordination numbers for rigid spheres of different size—estimating the number of next-neighbour interactions in a mixture, *Fluid Phase Equilibria*, 8 (1982) 123-129.
- [36] N. Rahmanian, Abd Ghani, N. , An investigation on process of seeded granulation in a continuous high shear granulator using DEM, in: *5th Asian Particle Technology Forum*, National University of Singapore, 2012, pp. 760-762.

List of Tables

Table 1: Geometry and material properties of the particles.

Table 2: Interactional properties used in the simulation.

Table 3: Geometrical properties of the granulator.

List of Figures

Figure 1: SEM image of seeded granules produced during the granulation experiments [15].

Figure 2: Regime map presented for production of seeded granule structure in Cyclomix granulator in which the probability of seeded granule formation is related to the impeller tip speed and the size ratio of seeds to fines (D_S/D_f) [12].

Figure 3: Force-overlap diagram in JKR model [26].

Figure 4: Schematic of the normal forces applied on a suspended particle due to adhesion and gravity.

Figure 5: Different views of the granulators used in the modelling. (a) Simple drum, (b) scooped drum.

Figure 6: Snapshots of simulation progress at two different simulation times for simple drum with 50 rpm rotational speed.

Figure 7: Total number of immediate contacts between seeds and fine particles in the granulator for different times.

Figure 8: Snapshots of granulation in the simple drum at different feeding stages and granulator rotational speeds.

Figure 9: Variation of total kinetic energy of particles and seed-fine contact number through time in the scooped and simple granulators.

Figure 10: Close up of the seeds having contacts with the fine granules in simple (left image) and scooped (right image) granulators. (t=10 s and rotational speed=50 rpm).

Figure 11: Number of fine particles needed to fully cover a seed with the size ratio of 4:1.

Figure 12: Effect of different granulator design on potential number of seeded granules.

Figure 13: Distribution of the percentage of seeds surface coverage at t=10 s.

Figure 14: Effect of different particle's surface energy on granule formation at speed of 50 rpm.

Figure 15: Front view snapshots of the granules inside the scooped drum for the tumbling speed of 50 rpm and the surface energies of 0.5, 1.5, 3, and 5 J/m².

Figure 16: Contact number per coordinate number for different seed-fine size ratios in a scooped granulator spinning with 30 rpm.

Figure 17: Distribution of the percentage of seeds surface coverage for different particles size ratios.

Table 1: Geometry and material properties of the particles.

Properties	Experiment @ 25°C	DEM modelling		Geometry
		Fine	Seed	
Particle size (mm)	0.043	1-2	8	---
Density (kg.m-3)	2750	800		7800
Poisson's ratio	0.2-0.3	0.2		0.29
Young's modulus (GPa)	69.9	0.24		200
Surface energy (J/m2)	0.043	0.50-5.00		0.50-5.00
Cohesion number	0.316	0.029-1.351		---

Table 2: Interactional properties used in the simulation.

Interaction	Particle-Particle	Particle –Geometry
Coefficient of restitution	0.2	0.2
Coefficient of static friction	0.6	0.7
Coefficient of rolling friction	0.1	0.1

Table 3: Geometrical properties of the granulator.

Parameter	Value
Volume of granulator (L)	~ 3.1
Length (mm)	400
Outer/ Inner Diameter (mm)	100/99
Gradient angle (rad)	0.05

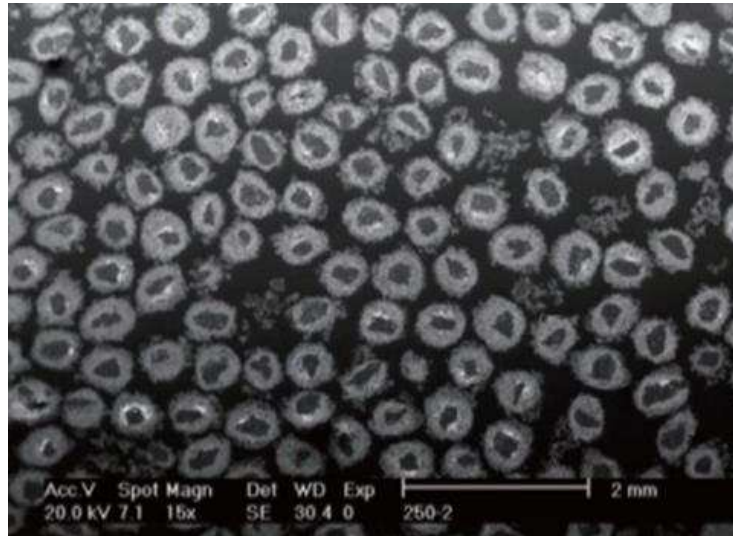


Figure 1: SEM image of seeded granules produced during the granulation experiments [15].

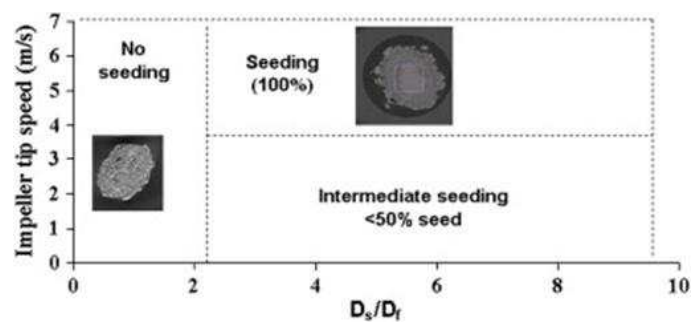


Figure 2: Regime map presented for production of seeded granule structure in Cyclomix granulator in which the probability of seeded granule formation is related to the impeller tip speed and the size ratio of seeds to fines (D_s/D_f) [12].

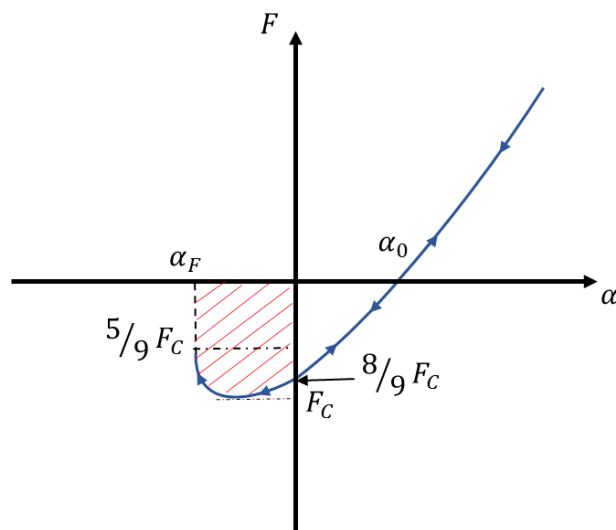


Figure 3: Force-overlap diagram in JKR model [26].

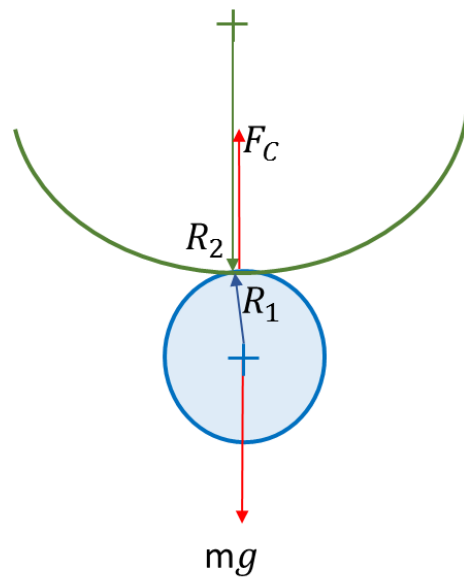


Figure 4: Schematic of the normal forces applied on a suspended particle due to adhesion and gravity.

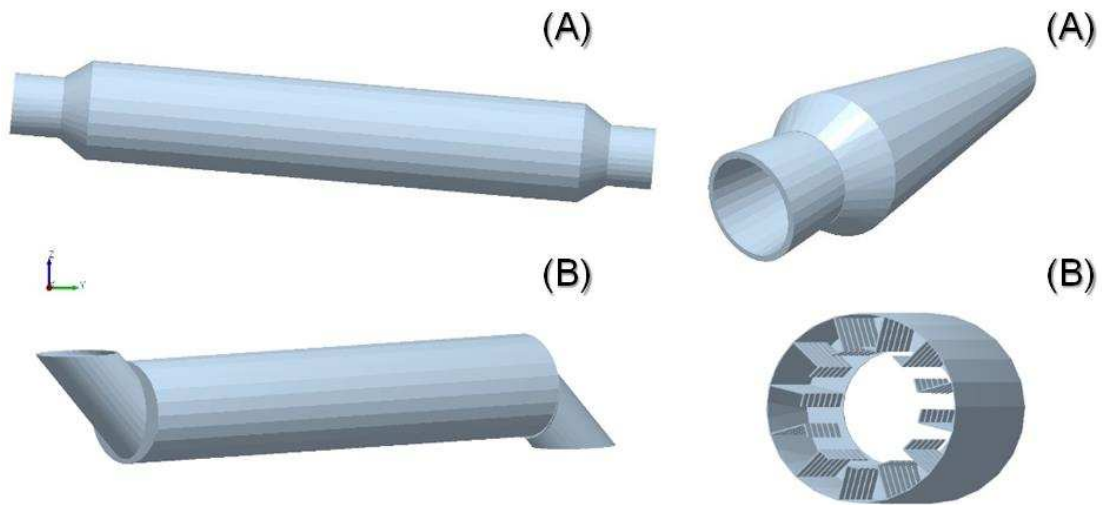


Figure 5: Different views of the granulators used in the modelling. (a) Simple drum, (b) scooped drum.

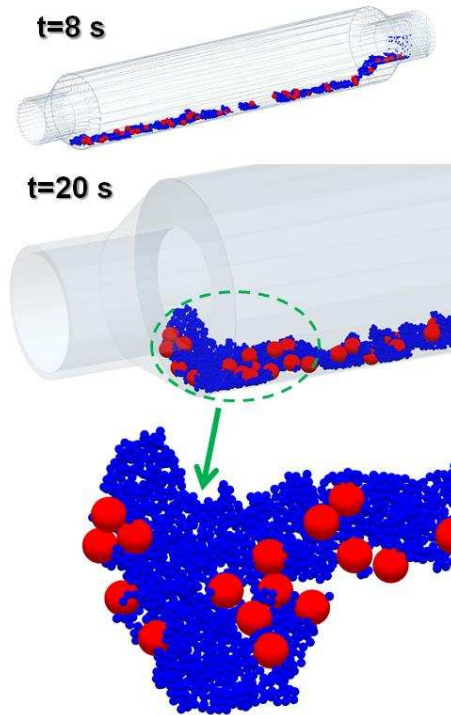


Figure 6: Snapshots of simulation progress at two different simulation times for simple drum with 50 rpm angular speed.

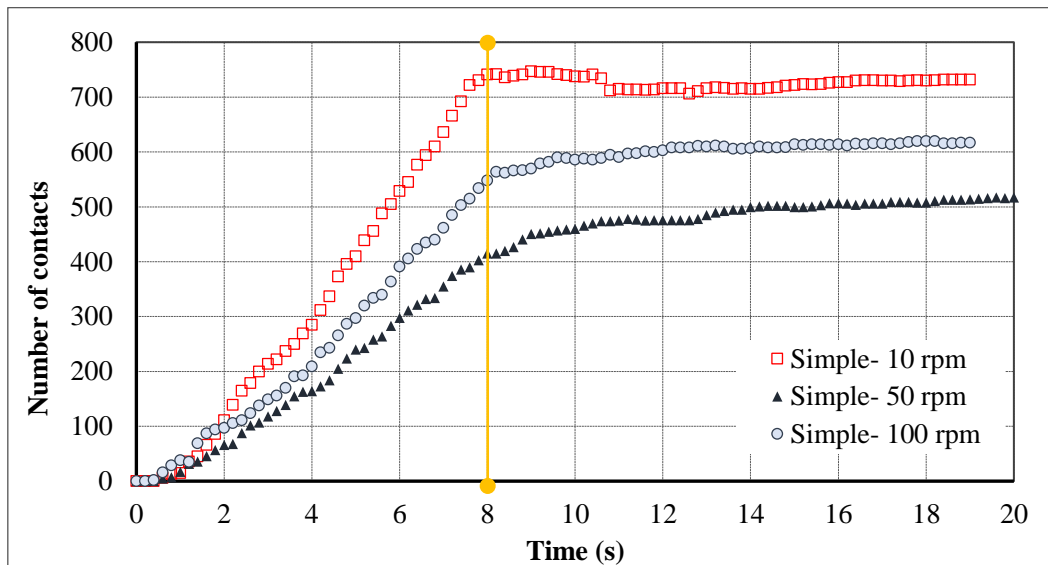


Figure 7: Total number of immediate contacts between seeds and fine particles in the granulator for different times.

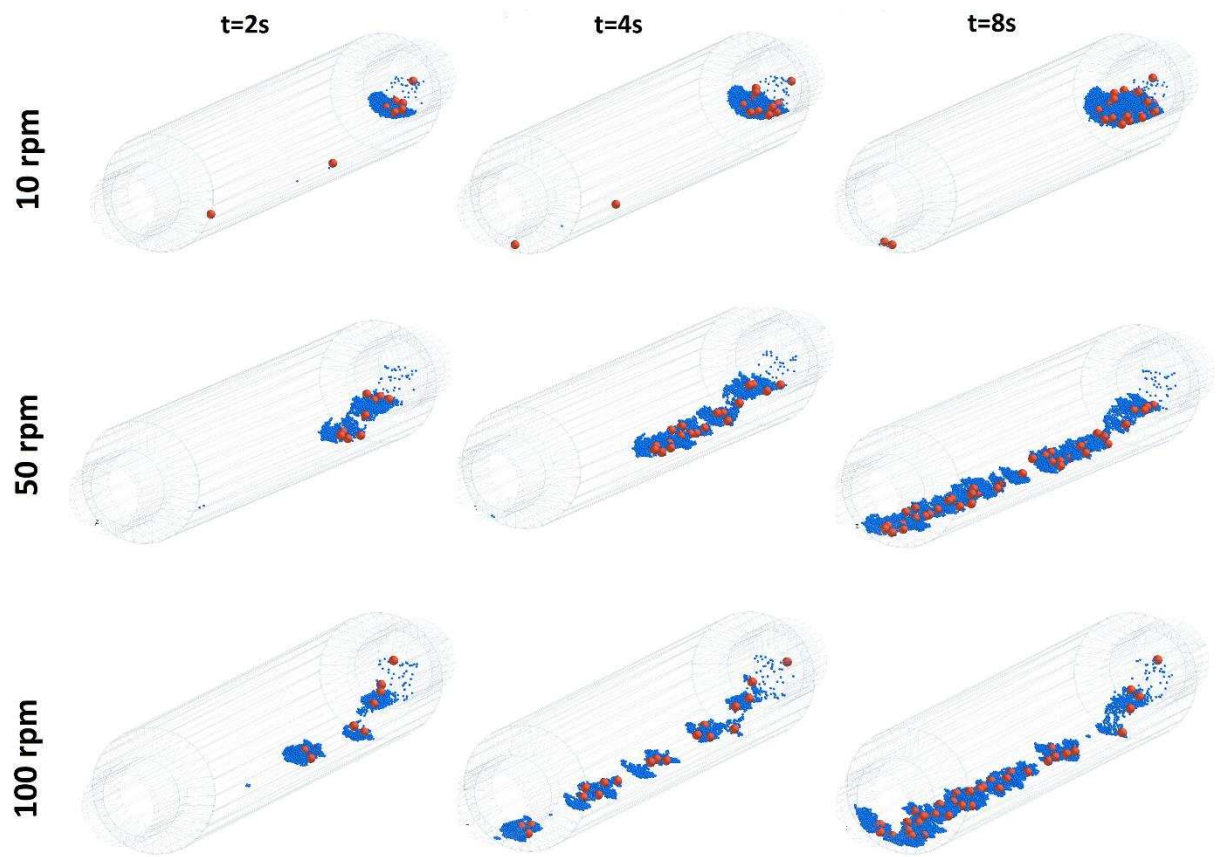


Figure 8: Snapshots of granulation in the simple drum at different feeding stages and granulator rotational speeds.

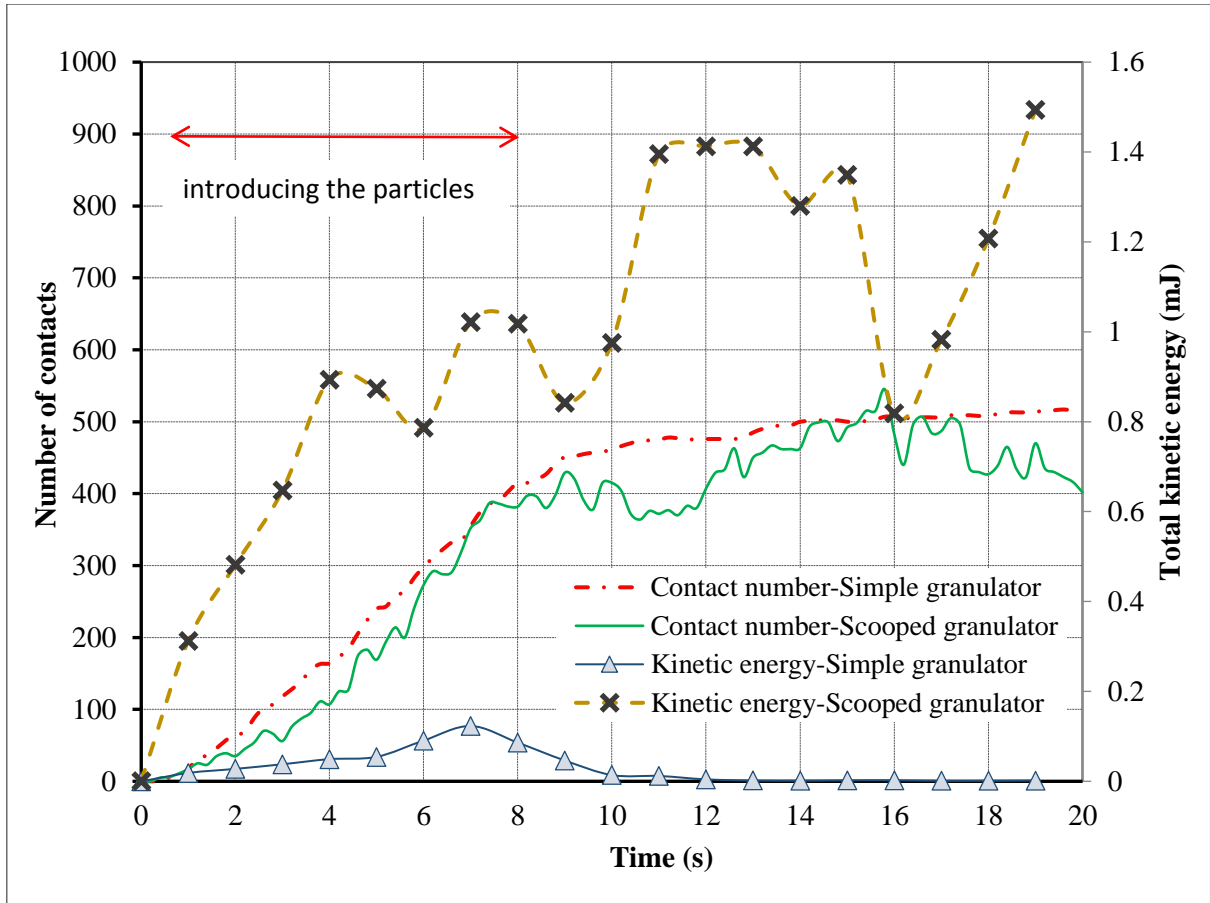


Figure 9: Variation of total kinetic energy of particles and seed-fine contact number through time in the scooped and simple granulators.

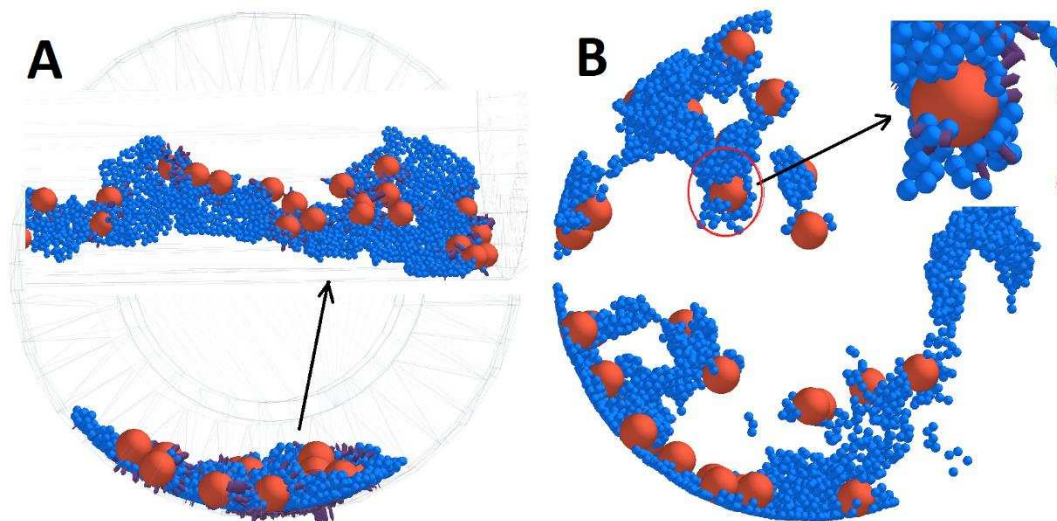


Figure 10: Close up of the seeds having contacts with the fine granules in simple (left image) and scooped (right image) granulators. ($t=10$ s and rotational speed=50 rpm).

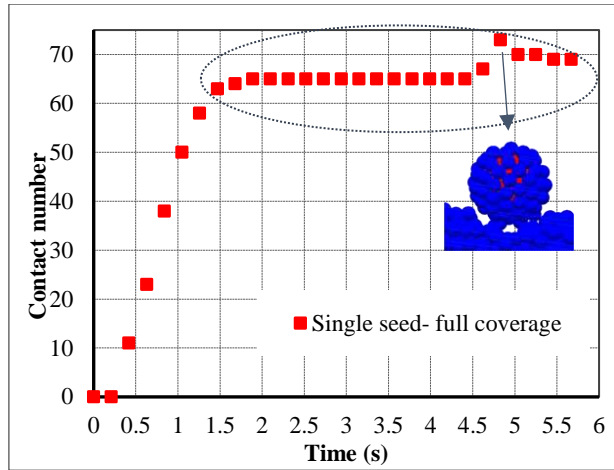


Figure 11: Number of fine particles needed to fully cover a seed with the size ratio of 4:1.

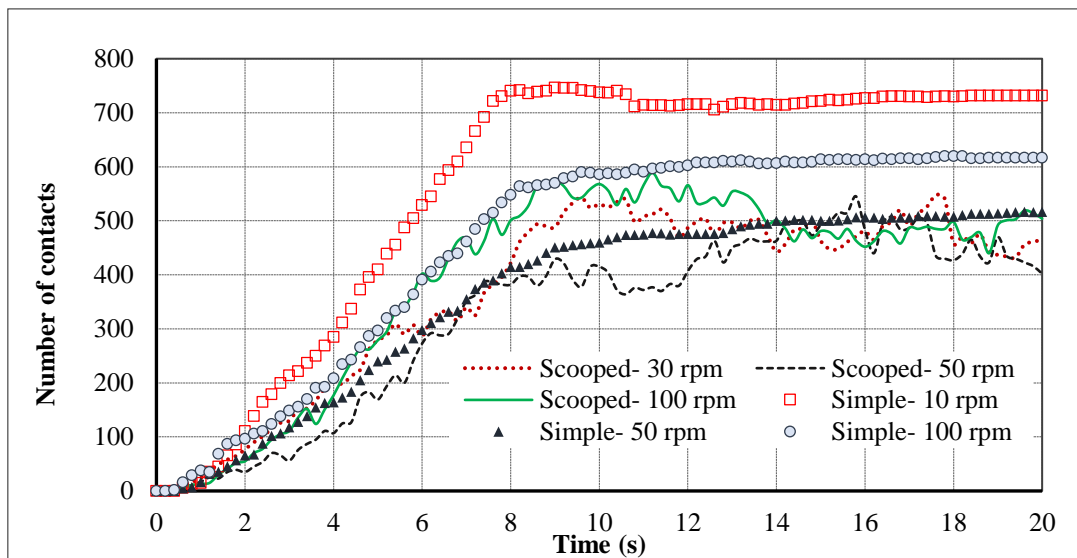


Figure 12: Effect of different granulator design on potential number of seeded granules.

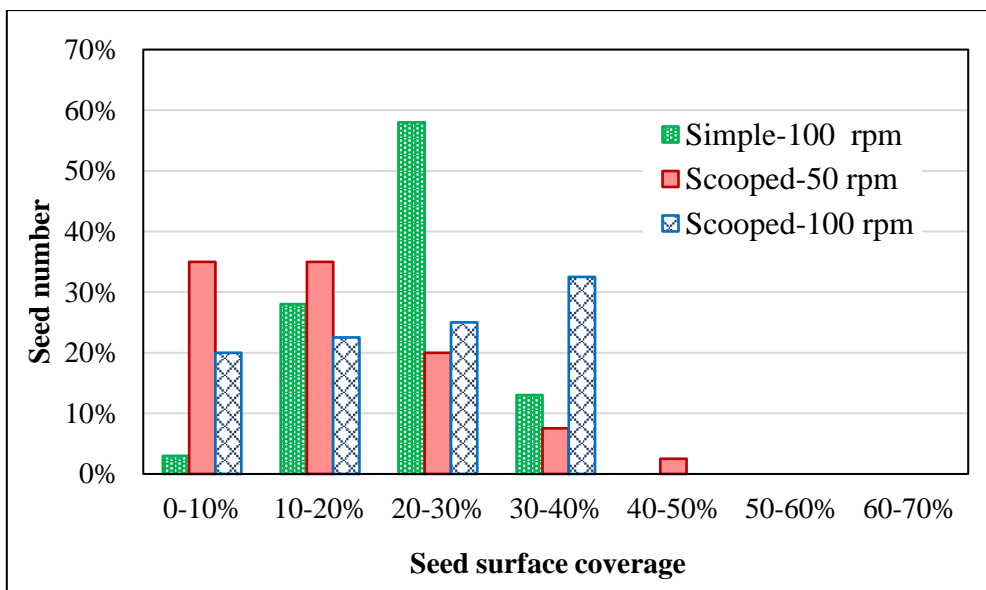


Figure 13: Distribution of the percentage of seeds surface coverage at t=10 s.

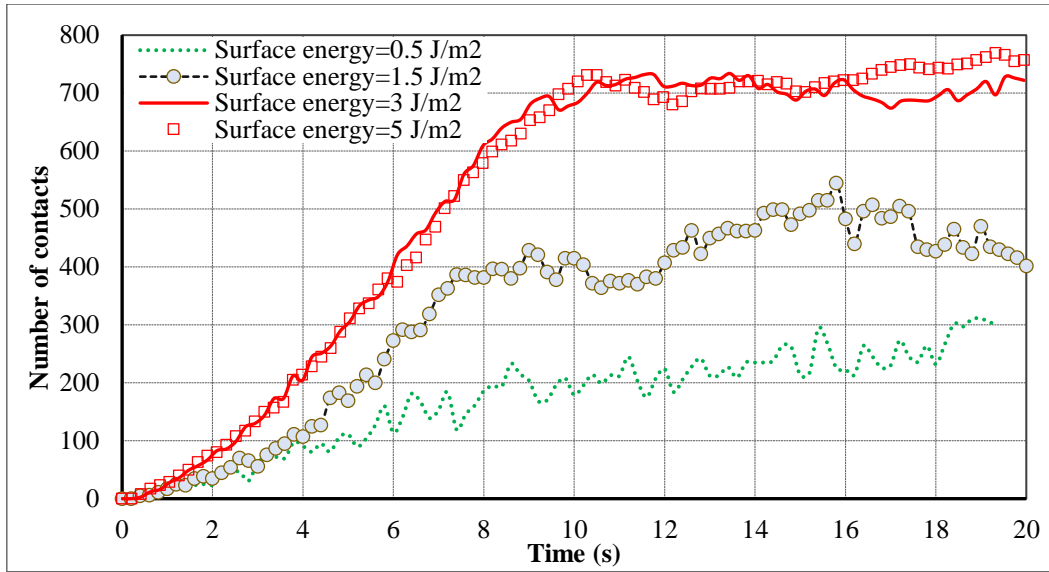


Figure 14: Effect of different particle's surface energy on granule formation at speed of 50 rpm.

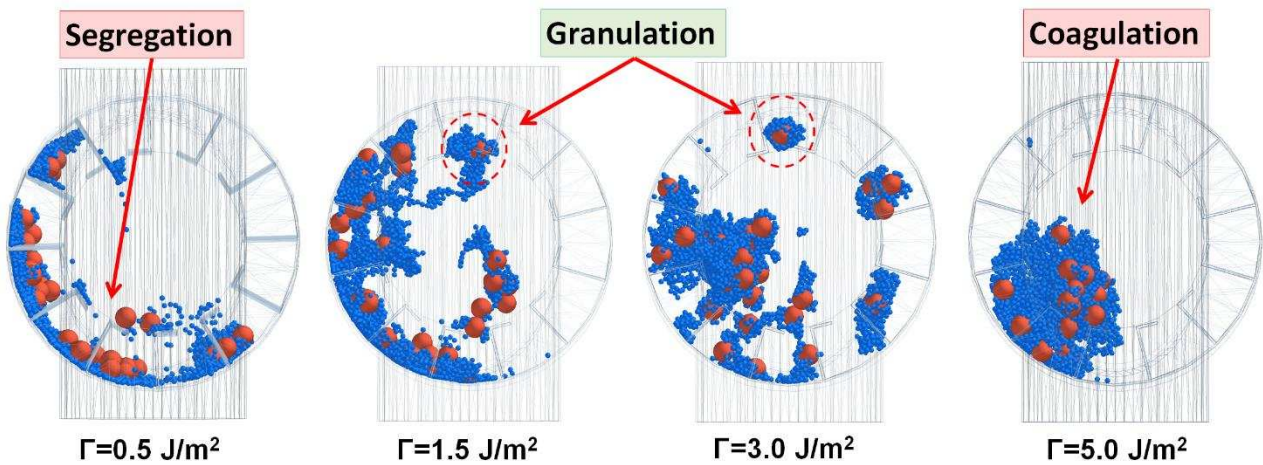


Figure 15: Front view snapshots of the granules inside the scooped drum for the tumbling speed of 50 rpm and the surface energies of 0.5, 1.5, 3, and 5 J/m².

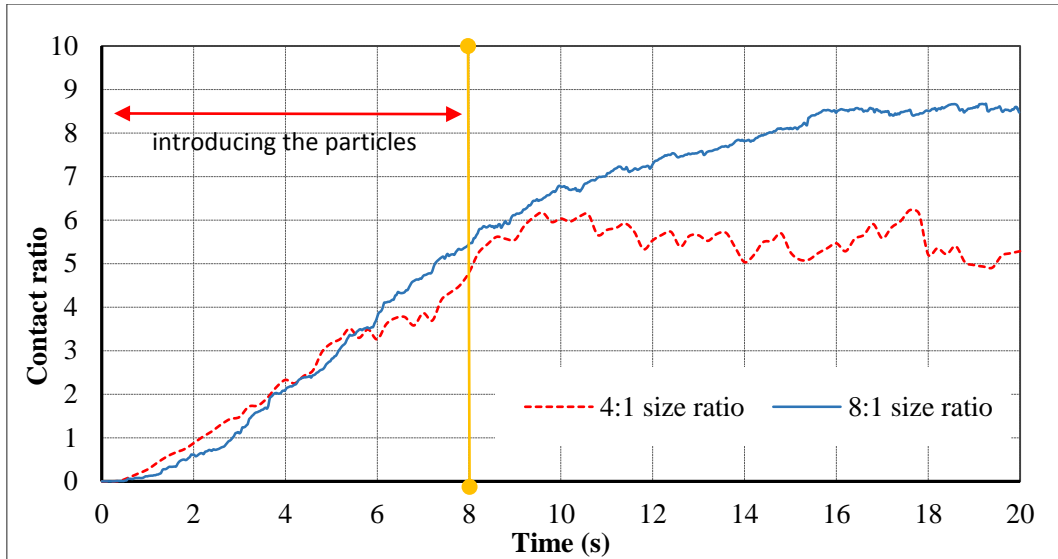


Figure 16: Contact number per coordinate number for different seed-fine size ratios in a scooped granulator spinning with 30 rpm.

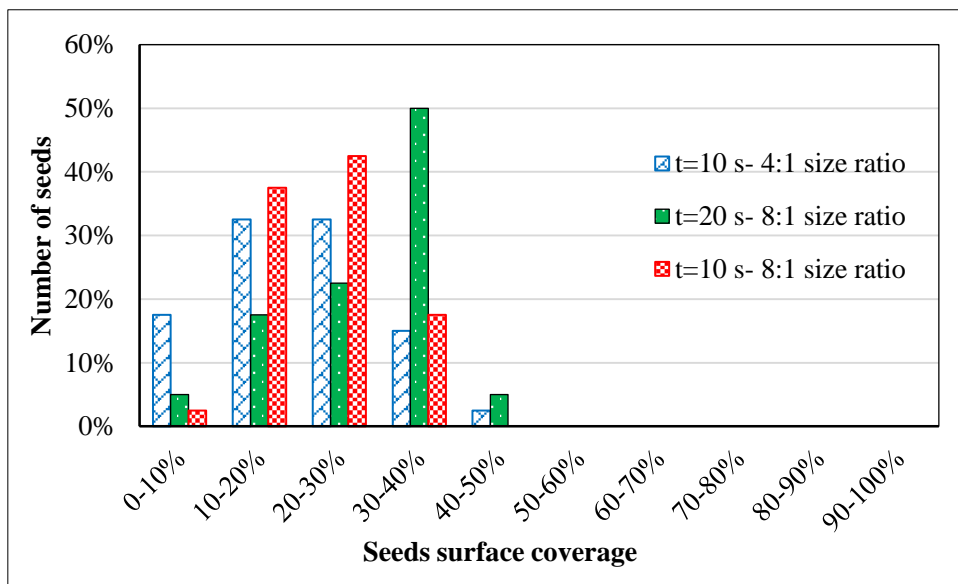


Figure 17: Distribution of the percentage of seeds surface coverage for different particles size ratios.